

COLLAGE: AUTOMATED INTEGRATION OF DEEP LEARNING BACKENDS

Byungsoo Jeon^{*1} Sunghyun Park^{*2} Peiyuan Liao¹³ Sheng Xu⁴ Tianqi Chen¹ Zhihao Jia¹

ABSTRACT

Strong demands for efficient deployment of Deep Learning (DL) applications prompt the rapid development of a rich DL ecosystem. To keep up with its fast advancement, it is crucial for DL frameworks to efficiently integrate a variety of optimized libraries and runtimes as their backends and generate the fastest possible executable by using them properly. However, current DL frameworks require significant manual effort to integrate diverse backends and often fail to deliver high performance. In this paper, we propose *Collage*, an automatic framework for integrating DL backends. *Collage* provides a backend registration interface that allows users to precisely specify the capability of various backends. By leveraging the specifications of available backends, *Collage* searches for an optimized backend placement for a given workload and execution environment. Our evaluation shows that *Collage* automatically integrates multiple backends together without manual intervention, and outperforms existing frameworks by $1.21\times$, $1.39\times$, $1.40\times$ on two different NVIDIA GPUs and an Intel CPU respectively.

1 INTRODUCTION

Due to the explosive popularity of Deep Learning (DL) applications, there are tremendous demands for high-performance software/hardware stacks that provide fast and efficient DL workload execution. These strong demands drive both industry and academia to invest a significant amount of effort in developing various cutting-edge hardware devices (Jouppi et al., 2017; ANE; NVD), optimized software libraries (Chetlur et al., 2014; One; Ten), and DL frameworks (Paszke et al., 2019; Abadi et al., 2016; XLA). Naturally, both hardware and software stacks have been diversified, resulting in a rich ecosystem.

Within this ecosystem, today’s DL frameworks can leverage a variety of highly optimized software libraries (Chetlur et al., 2014; Wang et al., 2014) and runtimes (Ten; Khan et al., 2019) as their *backends*¹ to deliver fast execution. Existing backends can be grouped into two categories based on their capabilities. The first category includes *operator libraries* (Chetlur et al., 2014; Wang et al., 2014; Khan et al., 2019) that lower individual DL operators (e.g., a convolution) to low-level kernel implementations. These libraries often provide sophisticated fusion engines (Chen et al., 2018; Chetlur et al., 2014; Niu et al., 2021) that follow certain fusion rules to allow complicated operator fusions. The second category covers *graph inference libraries* (Ten; One) that take an entire DL model as an input and optimize its execution by considering graph-level cross-kernel optimizations, such as scheduling and memory optimizations.

¹We define a *backend* as a software library or a runtime framework that takes DL workloads as inputs and generates an optimized low-level target code.

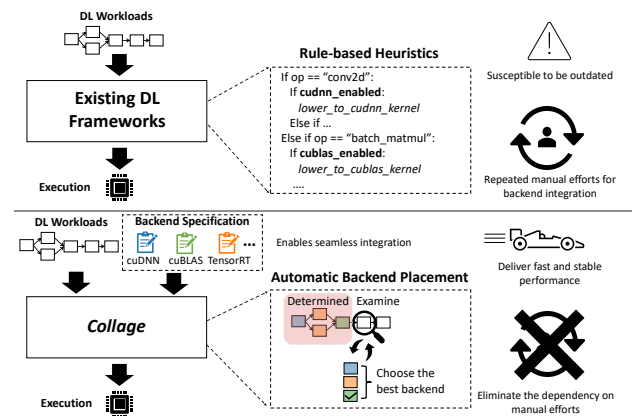


Figure 1. Different approaches for backend integration. Existing frameworks use rule-based heuristics to integrate different backends together. In contrast, *Collage* provides a backend specification interface to register all available backends and uses an automatic search algorithm to find optimized placement.

To effectively integrate diverse and fast-evolving backends in a DL framework, we must solve two problems: (1) incorporating a wide variety of available backends with different programming models and performance characteristics, and (2) optimizing placement of backends to effectively assign DL computations to various backends by leveraging the performance advantages of each backend. We call this overall problem **backend integration**.

Existing DL frameworks (Abadi et al., 2016; Paszke et al., 2019) use rule-based heuristics written by system experts (Figure 1) for backend integration. These heuristics often opportunistically offload the entire workload to the

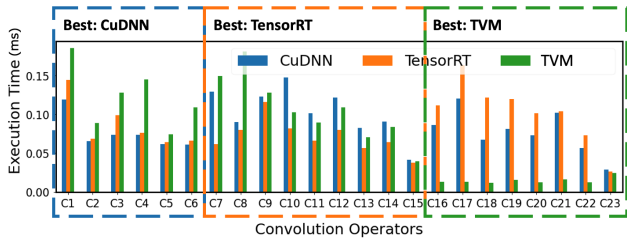


Figure 2. Performance of various convolutions with different configurations in ResNext-50 on NVIDIA RTX 2070; Note that there is no single *backend* that always delivers the fastest execution.

most promising single backend (e.g., a vendor-provided library). Otherwise, they lower each operator based on a fixed priority between backends. For example, cuDNN would have the highest priority for convolution, while cuBLAS would be the first choice for matrix multiplication. However, we observe that, even for the same type of operators, the optimal backend varies depending on an underlying execution environment (e.g., hardware) and input configuration (e.g., tensor shape, padding). Figure 2 demonstrates this observation. As a result, the manual approach in current DL frameworks may leave substantial performance on the table. Additionally, these handcrafted heuristics are hard to maintain and keep up with the rapid advancements in backends. Direct code modification to the framework is needed in order to introduce a new backend or reflect any updates from backend evolution.

In this paper, we propose to use an automated approach instead. In order to build such a solution, we need to solve two main challenges. First, it is non-trivial to integrate diverse backends with different characteristics into a system and leverage their full capability. Second, the search space of backend placements is extremely large since its size grows exponentially with the network size and the number of backends. The search space is further complicated by diverse backend capabilities and complicated fusion patterns.

To tackle these challenges, we build *Collage*, an automatic system for backend integration (Figure 1). Our system takes backend specifications along with a DL workload as inputs and effectively customizes DL executions without manual intervention. Our system contains two key components. First, to integrate diversified backends, we offer a descriptive operator pattern interface to specify the backend capability. We also provide a *pattern generator* to generate sophisticated patterns from a set of pattern rules. Second, to optimize backend placement, *Collage* employs a *two-level optimization* to deal with different characteristics of today’s operator and graph inference libraries. Our system explores possible matches between the input workload and operator patterns to find optimized placements by taking an underlying execution environment into consideration.

This paper makes the following contributions:

- We propose *Collage* to enable automated integration of diversified DL backends.
- We provide a pattern-based interface to enable quick registration of various backends without manually changing the core part of DL frameworks.
- We develop a two-level search method to optimize placement of diverse backends.

Our evaluation shows that *Collage* brings, on average, $1.21\times$, $1.39\times$, and $1.40\times$ speedup on two different NVIDIA GPUs and an Intel CPU respectively while removing the need of manual backend integration.

2 OVERVIEW

Figure 3 illustrates the overarching design of *Collage*, which takes a DL workload and specifications of backends as inputs, and optimize backend placement for the underlying hardware. *Collage* consists of two key components.

Backend Pattern Abstraction. Existing backends provide a variety of programming models for performing DL computations. To decouple backend capability from the placement algorithm and eliminate the manual effort for backend integration, we introduce *backend pattern*, a new abstraction for capturing the capability of varied backends. Specifically, a backend pattern defines a set of operators and their possible fusion combinations (e.g., Conv+ReLU) that can be deployed on each backend. Based on this pattern abstraction, our system provides a straightforward interface to register any backend and specify supported operator patterns.

Accurate specification is crucial to express the full capability of diverse backends. To achieve this, *Collage* offers two levels of abstraction. For simple patterns, *Collage* allows users to enumerate the supported operator patterns. However, this approach may not cover the full capability of backends with advanced fusion engines (Chen et al., 2018; Niu et al., 2021; Chetlur et al., 2014; Ten). To enable more flexible specification, *Collage* also allows users to bring their pattern rules that specify supported operator kinds and their complex operator fusions. When those rules are provided, the *pattern generator* automatically identifies all legitimate operator patterns on a given computation graph and adds them into the backend pattern registry. §3 provides details in depth.

Two-level Placement Optimizer. Once all available patterns are registered in the pattern registry, *Collage* uses a *two-level optimization* to discover an optimized backend placement for a given execution environment. As existing operator libraries offer operator-level point of view while graph inference libraries additionally apply cross-kernel op-

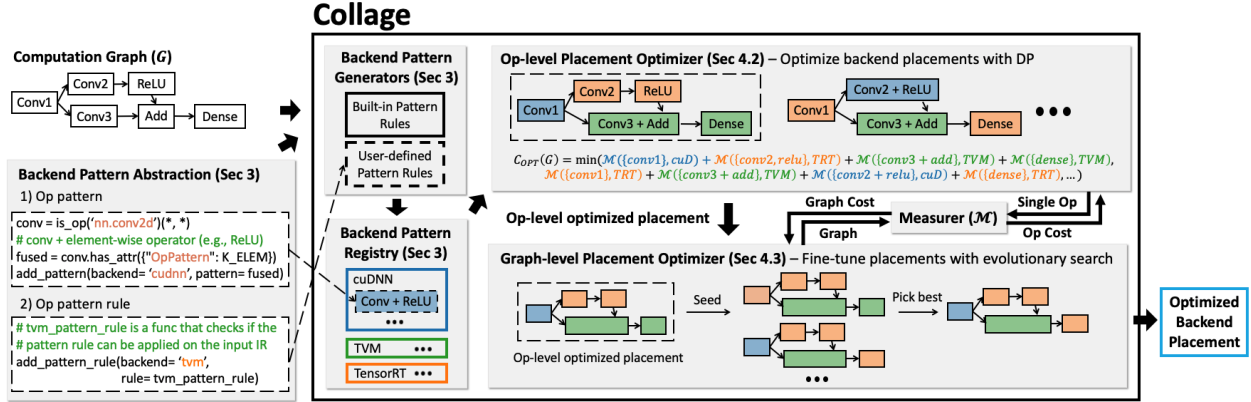


Figure 3. System overview of *Collage*. By using our backend specification interface, users can efficiently register diverse backend patterns supported by diverse backends. Then, with its two-level optimization process, *Collage* automatically optimizes backend placement for an underlying execution environment.

timizations, *Collage* takes two different optimization strategies to exploit their differences. First, an *op-level placement optimizer* explores promising candidates for individual operators, without considering cross-kernel optimizations. By adopting Dynamic Programming (DP), the op-level placement optimizer can efficiently find an optimized backend placement within a minute. Second, a *graph-level placement optimizer* will fine-tune the optimized backend placement using evolutionary search (Fortin et al., 2012). This compensates for the missing opportunities from the op-level placement optimizer by examining the impact of cross-kernel optimizations. §4 discusses the two optimizers in detail.

3 BACKEND PATTERN ABSTRACTION

As an important component of DL ecosystem, there are diverse fast-evolving backends with different programming models and performance characteristics. Depending on their target hardware and design principles, each backend has its own unique strength and coverage. In addition, many backends (Chetlur et al., 2014; Chen et al., 2018; Ten) support various complex operator fusions with sophisticated fusion engines (Chen et al., 2018; Niu et al., 2021), which add significant complexity in their integration with the full capability. Under the hood, existing operator fusion engines often fuse operators based on heuristic fusion rules that examine the type of each operation and the relationship between different types. For instance, a fusion engine may combine multiple operators across different branches into a single one as long as they satisfy its fusion rule.

For an adoption of various backends, our system provides two levels of abstraction: *pattern* and *pattern rule*. Pattern is a direct way to specify all supported operator patterns in *Collage*’s pattern language, which extends the Relay pattern language (Roesch et al., 2018). However, supported patterns

can be too complicated to explicitly specify. To incorporate sophisticated patterns, pattern rule offers a simple and flexible way to specify a valid set of operations and fusion rules in the form of Python functions. Each pattern rule is used to generate valid patterns for the input workload with our automatic pattern generator. With two levels of abstraction, users can easily incorporate an additional backend by specifying its patterns and pattern rules with an intuitive programming interface. *Collage* provides built-in patterns and pattern rules for popular backends (Chetlur et al., 2014; cuB; Ten; Wang et al., 2014; Chen et al., 2018).

Listing 1 presents an example of use-case scenarios. If a backend only supports a few simple patterns, users may enumerate those patterns and add them directly to the backend pattern registry (line 3-12). Users can easily check the operation (line 5), the relation between operators (line 7-8) and attributes, such as data layout or kernel size (line 6). Wildcard operator can be used as a special placeholder that matches any operator.

To fully support advanced backends (Chen et al., 2018; Niu et al., 2021; Chetlur et al., 2014; Ten), users can bring their pattern rules to incorporate more complicated patterns with *Collage*’s automatic pattern generator (line 14-48). To use this feature, users need to provide operation checkers with their potential constraints (line 15-24) and a fusion rule (line 26-43) in the form of Python function. Then, the automatic pattern generator in *Collage* will search for valid operator patterns satisfying these rules and add them to the backend pattern registry before the backend placement optimization starts.

Figure 4 exhibits how our pattern generator would search for legitimate patterns using given pattern rules on an input workload. By visiting every operator node in an input computation graph, the pattern generator investigates how far a

```

1 import collage
2
3 # [Method 1] Explicit pattern specification
4 # Pattern language to describe conv2d + add + relu.
5 conv = is_op('conv2d')(wildcard(), wildcard())
6 conv_constr = conv.has_attr({"data_layout": "NCHW"})
7 conv_add = is_op('add')(conv_constr, wildcard())
8 conv_add_relu = is_op('relu')(conv_add)
9
10 # Introduce new backend pattern to Collage.
11 collage.add_backend_pattern(backend='cuDNN',
12                             pattern=conv_add_relu)
13
14 # [Method 2] Pattern rule specification
15 # Checker for the supported operations.
16 def valid_op(op):
17     if op.name == "dense":
18         # Dense operation is always supported.
19         return True
20     elif op.name == "conv2d":
21         # constraints can be verified as well.
22         return op.attr["data_layout"] == "NCHW"
23     # ... rest of the op rule ...
24     return False
25
26 # Checker for fusion patterns.
27 # -- cur_type: type of current fusion group
28 # -- src: seed operator node
29 # -- sink: post-dominator of src
30 def fusion_rule(cur_type, src, sink):
31     %cur_type, src, sink = **kwargs
32     # If current fusion group contains
33     # at least one conv/matmul (kFusable)
34     if cur_type == kFusable:
35         # Helper functions can be defined.
36         def fchecker(node_pattern):
37             return (node_pattern == kElemwise)
38         # Check if every operator between src and sink.
39         # Helper function can be passed as a checker.
40         if collage.check_path(src, sink, fchecker):
41             return True
42     # ... rest of the fusion rule ...
43     return False
44
45 # Introduce new pattern generation rule to Collage.
46 collage.add_backend_pattern_rule(backend='TVM',
47                                 valid_ops=valid_ops,
48                                 fusion_rule=fusion_rule)
    
```

Listing 1: Example of the user interface for the backend specification. To register the backend capability in *Collage*, users can directly enumerate patterns or write a pattern rule that consists of valid operator checker and fusion rule in Python functions.

pattern can grow without breaking the pattern rule. At each operator node, the pattern generator verifies the current node by using the operation checker of a backend (line 15-24). If valid, it enlarges the scope one step further and validates whether a set of nodes satisfies the fusion rule (line 26-43). For instance, line 34-41 specify that the assumed backend can fuse element-wise operators followed by an operator of type `kFusable`, which includes convolution and matrix multiplication. Whenever a group of operators satisfying the rule is found, the pattern generator produces a corresponding pattern and adds it to the backend pattern registry. Then, it enlarges the scope of interests one step further again to see if a bigger pattern can be found. This approach allows

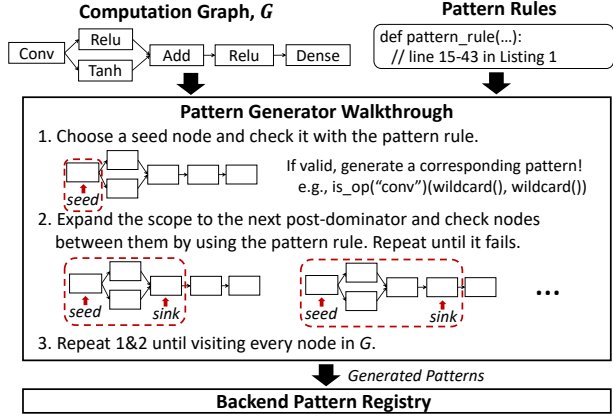


Figure 4. Example illustrating how the backend pattern generator would automatically generate valid patterns with the pattern rule presented in Listing 1.

Collage to incorporate advanced backends, such as TVM, cuDNN, DNNL and TensorRT, without any missing pattern.

4 BACKEND PLACEMENT OPTIMIZATION

4.1 Problem Definition

To maximize the performance by finding the best use of available backends, *Collage* focuses on the backend placement problem. Consider a computation graph \mathcal{G} and a set of backend patterns \mathcal{B} in *Collage*'s backend pattern registry. Note that \mathcal{G} is a Directed Acyclic Graph (DAG) where each node represents a tensor operator (e.g., convolution, matrix multiplication). With M matched subgraphs g_i and backend patterns b_i for $i = 1 \dots M$, let $\mathcal{P}(\mathcal{G}) = \{(g_i, b_i) | b_i \in \mathcal{B}, \bigcup_{i=1}^M g_i = \mathcal{G}, g_i \cap g_j = \emptyset \text{ for all } i, j \in \{1, 2, \dots, M\} \text{ where } i \neq j\}$ be a backend placement on a computation graph \mathcal{G} and $Cost(\mathcal{P}(\mathcal{G}))$ be the run-time cost (e.g., execution time) function of a placement $\mathcal{P}(\mathcal{G})$. In this work, we aim to find a backend placement $\mathcal{P}(\mathcal{G})$ that minimizes $Cost(\mathcal{P}(\mathcal{G}))$. This problem can be formalized as follows:

$$\mathcal{P}_{opt}(\mathcal{G}) = \arg \min_{\mathcal{P}(\mathcal{G})} Cost(\mathcal{P}(\mathcal{G})) \quad (1)$$

With the two-level optimization, *Collage* endeavors to optimize the backend placement by searching for \mathcal{P}_{opt} .

4.2 Op-level Placement Optimizer

To enable the cost-efficient evaluation of a graph with a backend placement candidate and prune the search space effectively, *Collage* conducts an op-level placement optimization as the first step. Its goal is to map all operators on the computation graph to the most efficient set of low-level kernel implementations from available backends without

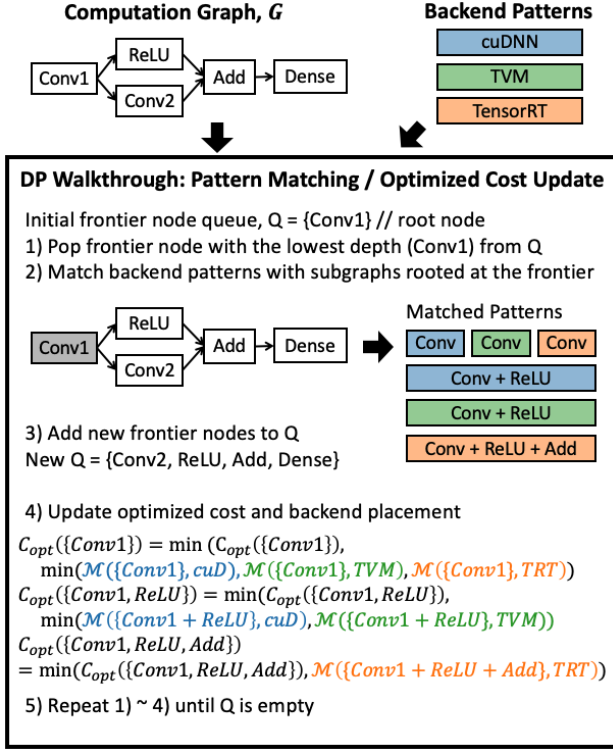


Figure 5. Example of Dynamic Programming (DP) procedures. By visiting over each frontier node, DP algorithm matches backend patterns and update the optimized placement and its cost. For simplicity, optimized placement update is omitted.

considering cross-kernel optimizations in graph inference libraries. As discussed earlier, the graph-level placement optimizer (§4.3) would make up for the possible performance loss from this simplification.

With this simplification, low-level kernel executions become independent to each other in a single device execution. Let s_1 and s_2 be subgraphs of \mathcal{G} where $s_1 \cup s_2 = \mathcal{G}$, $s_1 \cap s_2 = \emptyset$. Then, the following additive relationship (Jia et al., 2019a) between run-time cost of $\mathcal{P}(s_1)$ and $\mathcal{P}(s_2)$ can be used to determine $Cost(\mathcal{P}(\mathcal{G}))$:

$$Cost(\mathcal{P}(\mathcal{G})) = Cost(\mathcal{P}(s_1)) + Cost(\mathcal{P}(s_2)) + \epsilon \quad (2)$$

where ϵ is a constant for context switching cost. With this cost model, it is possible to cheaply approximate the cost of a graph by partitioning a graph into smaller subgraphs and summing up their cost. Despite the efficient cost model, excessively large number of possible placements and a variety of fusion patterns make search challenging.

To address this challenge, we propose a Dynamic Programming (DP) method for the op-level placement optimization. By using the additive relation (Equation 2), we deduce the following recurrence relation of optimized backend placement $\mathcal{P}_{opt}(s)$ and its cost $C_{opt}(s)$ for any subgraph $s \subset \mathcal{G}$.

Algorithm 1 Op-level Placement Optimization: DP

Input: Computation graph \mathcal{G} and set of backend patterns \mathcal{B}
Output: Optimized placement $\mathcal{P}_{opt}(\mathcal{G})$

```

1: //  $v_0$ : a root of  $\mathcal{G}$ ,  $Q$ : a priority queue sorted by node depth
2:  $Q = \{v_0\}$ 
3: repeat
4:    $v_s = Q.dequeue()$ 
5:   for  $b_i \in \mathcal{B}$  do
6:     if  $b_i$  matches any subgraph  $g$  rooted at  $v_s$  then
7:       //  $\mathcal{F}$  is a set of new frontier nodes after matching
8:       for  $v_j \in \mathcal{F}$  do
9:         if  $v_j$  has never been added to  $Q$  then
10:            $Q.enqueue(v_j)$ 
11:         end if
12:       end for
13:
14:       //  $\mathcal{P}(g) = \{(g, b_i)\}$ 
15:       //  $\mathcal{M}$  is a measurer
16:       //  $\mathcal{S}$  is a set of subgraphs, each of which includes all nodes before  $v_s$ 
17:       //  $\epsilon$  is a constant for context switching cost
18:       for  $s_j \in \mathcal{S}$  do
19:         if  $C_{opt}(s_j \cup g) > C_{opt}(s_j) + \mathcal{M}(\mathcal{P}(g)) + \epsilon$  then
20:            $C_{opt}(s_j \cup g) = C_{opt}(s_j) + \mathcal{M}(\mathcal{P}(g)) + \epsilon$ 
21:            $\mathcal{P}_{opt}(s_j \cup g) = \mathcal{P}_{opt}(s_j) \cup \mathcal{P}(g)$ 
22:         end if
23:       end for
24:     end if
25:   end for
26: until  $Q = \emptyset$ 
27:
28: return  $\mathcal{P}_{opt}(\mathcal{G})$ 
    
```

This breaks down a problem of finding $\mathcal{P}_{opt}(\mathcal{G})$ into smaller problems of finding $\mathcal{P}_{opt}(s)$.

$$\mathcal{P}_{opt}(s) = \mathcal{P}_{opt}(s_{min}) \cup \mathcal{P}(g_{min})$$

$$C_{opt}(s) = \begin{cases} 0 & \text{if } s = \emptyset \\ C_{opt}(s_{min}) + \mathcal{M}(\mathcal{P}(g_{min})) + \epsilon & \text{otherwise} \end{cases} \quad (3)$$

where s_{min} and g_{min} are

$$\arg \min_{s' \cup g' = s, s' \cap g' = \emptyset} \{C_{opt}(s') + \mathcal{M}(\mathcal{P}(g')) + \epsilon\} \quad (4)$$

s' represents a subgraph that is already examined while g' is a subgraph that is going to be evaluated with a measurer $\mathcal{M}(\cdot)$. The measurer takes a backend placement and returns its actual run-time cost on the execution environment. We query the measurer at the granularity of a backend pattern that matches with g' , which is either single or multiple operators (operator fusion) that will be lowered to the single low-level kernel. This ensures that we always measure a single kernel and add it up to compute the cost of larger subgraphs. To avoid the repetitive and expensive measurement overhead (i.e., compilation + multiple runs on the actual

hardware), we cache the result to the log for the future usage. With this approach, we can efficiently explore possible backend placements and evaluate them. Algorithm 1 formalizes our DP method.

Figure 5 illustrates an walkthrough example of our DP method. By traversing a computation graph \mathcal{G} , it solves smaller problems of finding $\mathcal{P}_{opt}(s)$ for a subgraph $s \subset \mathcal{G}$ and eventually discover $\mathcal{P}_{opt}(\mathcal{G})$. First, it puts a root node in the priority queue as an initial frontier node; we define a *frontier node* as a node that has the lowest depth among unvisited nodes on a path from the root. Then it pops a frontier node with the lowest depth from the queue and examines if any subgraph rooted at the current frontier node can match any valid backend pattern. Once matching is found, we add new frontier nodes to the priority queue and measure the cost of subgraph matched with the backend pattern. If better placement is found, we update the optimized cost and backend placement based on Equation (3). We repeat these steps until the priority queue is empty. Note, given that graph inference library, such as TensorRT, can also provide competitive operator-level implementations (Figure 2), we also include them in the op-level optimization.

4.3 Graph-level Placement Optimizer

As the op-level placement optimization ignores the effect of cross-kernel optimizations (e.g., scheduling and memory optimizations) in graph inference libraries, *Collage* introduces the graph-level optimization to fine-tune the potentially sub-optimal backend placements from the op-level. To do so, we need to identify additional operators that are not assigned to graph inference libraries but can benefit from cross-kernel optimizations. Once identified, we offload them to graph inference libraries to extract the further speedup. However, it is a challenging problem as it is non-trivial to decide which operators to offload to graph inference libraries among a myriad of candidates.

For the effective search, we represent each backend placement state by using a sequence of digits. Each digit implies whether to offload to graph inference libraries or not. Since our goal is to offload more operators that can benefit from the cross-kernel optimization, we exclude operators that are already mapped with the graph inference library from the sequence of digits. Fused operators will be checked whether those can also be offloaded to graph inference library. If so, they will be considered as a group and a single digit will represent them in the sequence. Otherwise, each operator will have separate digits in the sequence. This straightforward state representation eliminates the complexity from various graph partitions and their topology.

With this search space, we adopt evolutionary search algorithm (Fortin et al., 2012) for graph-level placement optimization. Figure 6 describes the procedure of our evolution-

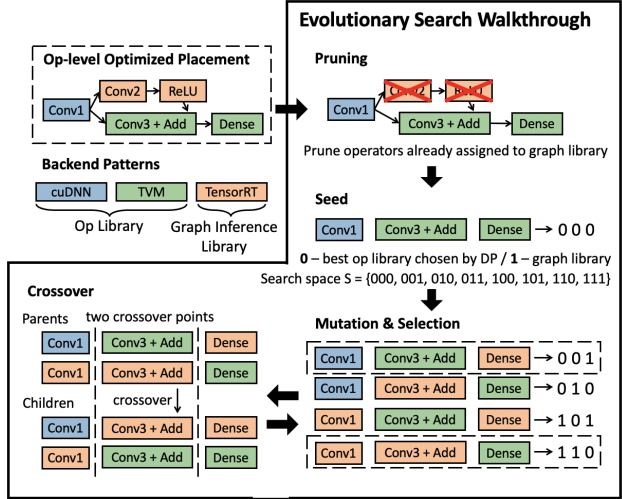


Figure 6. Example of Evolutionary Search (ES) procedure. After pruning search space, it iterates over mutation, selection, and crossover until it reaches saturation or predefined time limit.

ary search method. For state representation example, we assume 0 as keeping the decision from the op-level and 1 as overriding the decision and offload it to graph inference library (e.g., TensorRT). To facilitate the search process, we include the op-level optimized placement as one of the seeds to provide a good starting point. The evolutionary algorithm iterates over rounds of mutation, selection, and two-point crossover to fine-tune the backend placement.

5 RELATED WORK

Diversified Backend Ecosystem. To extract the best performance from the underlying hardware, there have been substantial efforts to design high-performance backends. Hardware vendors have released various specialized optimized libraries and inference engines. NVIDIA has actively developed cuDNN (Chetlur et al., 2014) to deliver optimized implementations of DL operators, cuBLAS (cuB) to offer efficient BLAS kernels, and TensorRT (Ten) to create the fast execution plan for DL workloads. Particularly, TensorRT considers various graph-wide cross-kernel optimizations for scheduling, memory footprint and etc. Meanwhile, Intel has released oneDNN (One) for optimized DL operator kernels and openVINO (Ope) as an inference engine for Intel CPUs. AMD also has driven MIOpen (Khan et al., 2019) which is an open source GPU library for DL primitives. We can also consider tensor compilers as backends (Ragan-Kelley et al., 2013; Adams et al., 2019; Chen et al., 2018; Baghdadi et al., 2019; Fegade et al., 2021; Zheng et al., 2020a; Lattner et al., 2021) that provide optimized operator kernels for various target devices. To intelligently deal with the fast-evolving backend diversity, *Collage* provides the user interface and

two-level optimization to enable efficient integration of various backends and automatically find their best uses given their unique strengths.

DL Frameworks. To provide easy and powerful platform of running a variety of DL workloads, different frameworks have been continuously released and improved. Google maintains TensorFlow (Abadi et al., 2016) and XLA (XLA) to optimize the execution on various hardware devices including TPUs (Jouppi et al., 2017). Facebook develops Pytorch (Paszke et al., 2019) that supports dynamic eager execution for usability while preserving compelling DL execution performance. For NVIDIA GPUs, TensorRT (Ten) is developed as a runtime framework that optimizes DL model execution. As an open-source C++ library and compiler suite for CPUs, Intel has launched nGraph (Cyphers et al., 2018). Also, TVM (Chen et al., 2018) offers the efficient compilation pipeline that is designed to support diverse hardware devices and DL workloads. On the other hand, Glow (Rotem et al., 2018) is proposed to efficiently generate the optimized code for multiple targets of heterogeneous hardware. While the existing DL frameworks employ handwritten rules to integrate new backend, we suggest an automated integration solution that eliminates the manual effort and extracts better performance.

Operator Fusion. Fusion is one of the most efficient techniques to optimize DL workloads by combining multiple high-level operators on the computation graph into a single kernel. To maximize the benefit, advanced fusion techniques introduce their own unique fusion rules to apply this optimization beyond a few special cases. For instance, by iterating over every operator in the workload, TVM endeavors to seek for an opportunity to merge each operator with its neighbors by using the union-find algorithm (Chen et al., 2018). To efficiently explore the fusion opportunities, DNN-Fusion employs a detailed classification of operation type and makes the fusion decisions. To identify the best fusion plan, FusionStitching conducts Just-In-Time tuning (Zheng et al., 2020b). NVIDIA has actively improved the fusion engine in cuDNN to merge certain patterns of operators at runtime (Chetlur et al., 2014). Internally, TensorRT also actively apply the fusion to optimize the memory access and scheduling overhead (Ten). By offering the highly flexible user interface for the pattern rules, *Collage* can support such complicated fusion patterns from a variety of backends.

Graph Rewriting. To accelerate a DL execution, DL frameworks can rewrite an input computation graph by considering a number of graph substitution rules. Most DL frameworks such as TensorFlow (Abadi et al., 2016), TensorRT (Ten), and TVM (Chen et al., 2018) rely on the greedy approach by opportunistically applying a few important hand-coded rules. In contrast, MetaFlow (Jia et al., 2019b) suggests an automated graph rewriting approach

that optimizes an input graph using backtracking search. TASO (Jia et al., 2019a) extends MetaFlow’s backtracking search and further automates graph substitution generation for every new input graph. To further improve graph substitution search efficiency, sampling-based approach (Fang et al., 2020) has also been explored. However, (Yang et al., 2021) points out the inefficiency in making sequential rewriting decisions and resolves this issue by proposing e-graph and equality saturation method. As these graph rewriting techniques are orthogonal to *Collage*, *Collage* can improve the performance of a rewritten computation graph by optimizing the backend placement .

6 EVALUATION

This section aims to answer the following questions:

- Can *Collage* effectively optimize real-world DL model execution over diverse backends and target devices compared to the existing DL frameworks? (§6.2)
- Is optimization time affordable? How much time does each optimization take? (§6.3)
- Does adding more backends improve the performance of *Collage*? (§6.4)
- How does backend placement optimized by *Collage* look like? (§6.5)

6.1 Experimental Setup

We implement the core of *Collage* in the form of a portable Python library and leveraged diverse backends in different hardware architectures: cuDNN (Chetlur et al., 2014), cuBLAS (cuB), TVM (Chen et al., 2018), TensorRT (Ten), MKL (Wang et al., 2014) and DNNL (One). To leverage their full capabilities, their supported patterns and pattern rules are provided based on their official documentation and code bases. It takes us to write about 70 lines of codes to integrate each backend. TensorFlow (TF) (Abadi et al., 2016), TF-XLA (XLA), PyTorch (Paszke et al., 2019), TVM (Chen et al., 2018), and TensorRT (Ten) are examined as DL framework baselines. Note that we also integrate TensorRT and TVM as backends to our system as they are known to be high-performance.

We evaluate five popular real-world DL workloads that cover a wide range of application. BERT (Devlin et al., 2018) is a transformer-based language model that achieved the state-of-the-art performance on a spectrum of natural language processing tasks. DCGAN (Radford et al., 2015) is an extension of the GAN (Goodfellow et al., 2020) with an unsupervised representation learning mainly for image generation. NasNet-A (Zoph et al., 2018) is one of the

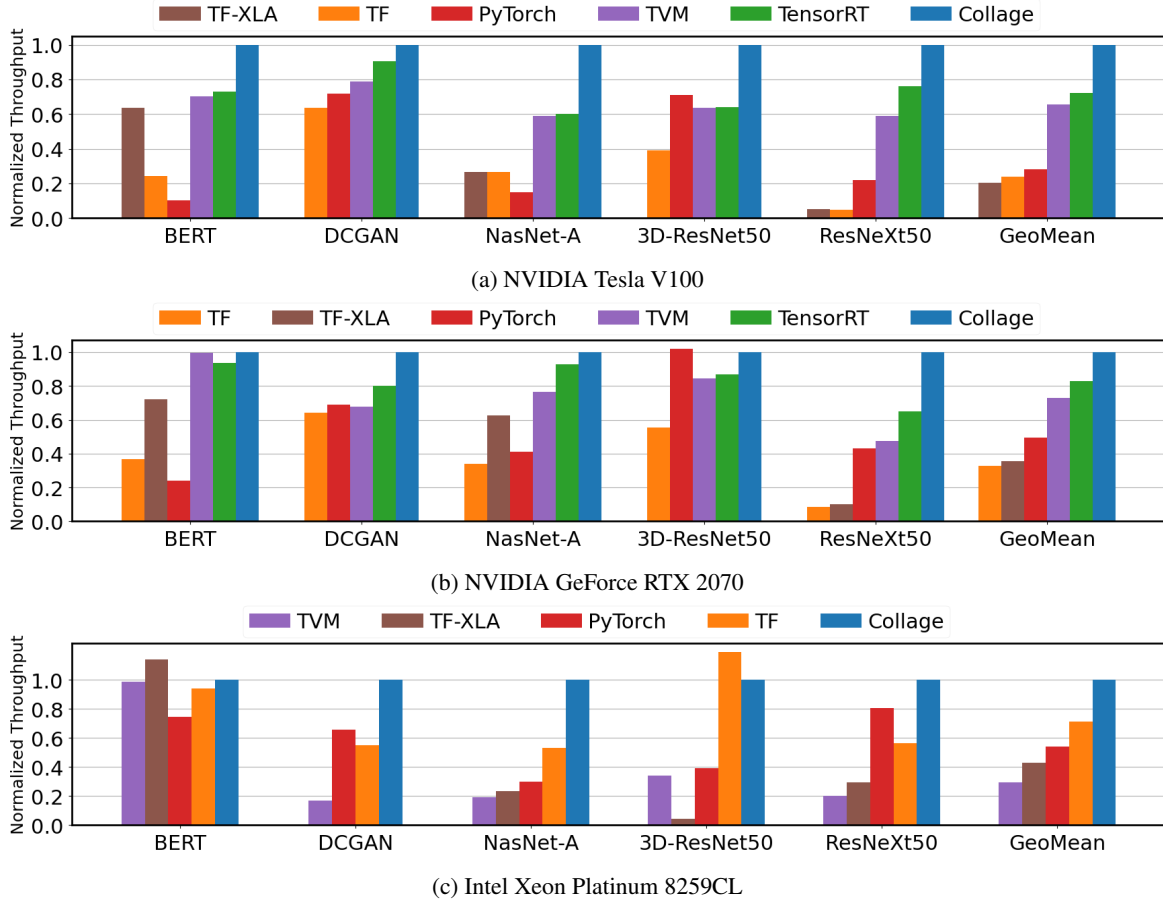


Figure 7. End-to-end performance of state-of-the-arts DL frameworks and *Collage* in five real-life workloads on NVIDIA GPUs and Intel CPU. Throughput of each framework is normalized by the throughput of *Collage*. Following backends are employed for each framework according to target hardware and its capabilities: NVIDIA GPU (cuDNN, cuBLAS, TVM, TensorRT), Intel CPU (MKL, DNNL, TVM).

most popular machine-generated DL workloads that show strong performance on popular image recognition tasks. 3D-ResNet50 (Hara et al., 2018) is an extension of widely adopted ResNet50(He et al., 2016) for 3D image tasks such as action recognition. ResNeXt50 (Xie et al., 2017) introduces a grouped convolution to ResNet50 architecture and improves its model accuracy and computational complexity for image recognition.

6.2 End-to-end Evaluation

To discuss the effectiveness of our automated approach, we evaluate the end-to-end performance of *Collage* against the baseline frameworks.

Figure 7a and Figure 7b presents the end-to-end normalized throughput of *Collage* and existing DL frameworks on two different NVIDIA GPU architectures, Tesla V100 and GeForce RTX2070. Normalized throughput is the throughput of each framework normalized by the throughput of *Collage*. Overall, *Collage* consistently produces the most ef-

ficient executable across different workloads and hardware architectures: In terms of geometric mean, *Collage* outperforms the state-of-the-arts by $1.39\times$ on V100 and $1.21\times$ on RTX 2070, respectively. This improvement comes from *Collage*'s backend placement optimization that effectively leverages the unique strength of various backends specified by our backend pattern abstraction.

Figure 7c exhibits the experimental results on the Intel CPU. Likewise, *Collage* showcases the most stable performance across different workloads on this Xeon architecture while beating the state-of-the-arts by $1.40\times$ in the geometric mean. However, on BERT and 3D-ResNet50, TF-XLA and TF are faster possibly due to their different optimization pipeline, which is orthogonal to backend placement.

As the representative case, different batch sizes are also examined with ResNeXt50 on V100. Figure 8 indicates that *Collage* consistently outperforms the state-of-the-art frameworks across different batch sizes as well.

Since backends and their performance vary depending on

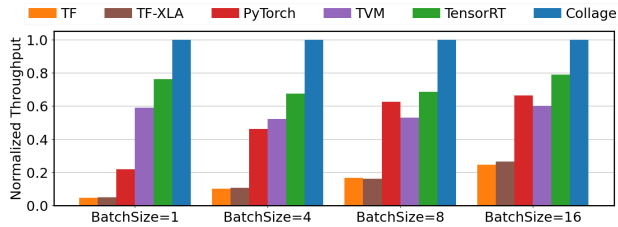


Figure 8. End-to-end performance with different batch sizes in ResNeXt50 on NVIDIA V100. Normalized throughput is the throughput normalized by the throughput of *Collage*.

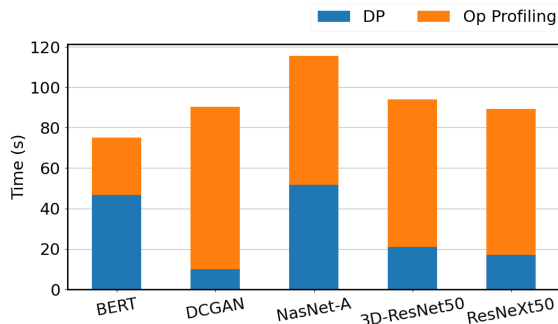


Figure 9. The breakdown of op-level placement optimization time. On average, profiling overhead for operator cost measurements takes up 68% of the entire optimization time. Note that profiling is only necessary for unseen operators. Once the cost of a new operator is measured, its information will be saved in the logging database in *Collage* to avoid the repetitive profiling.

the underlying execution environment, backend placement should be carefully customized by considering their performance landscape. Our experimental results indicates that *Collage* with the automated solution can stably offer a faster DL execution than existing frameworks with the rigid hand-written heuristics across different hardware architectures.

6.3 Optimization Time

To evaluate the overhead from our automated solution, this subsection studies the overall optimization cost of the two-level approach.

Figure 9 shows the breakdown of our operator-level optimization time. If the optimization is launched from scratch, the entire optimization process takes up to two minutes. This optimization time consists of two parts: measurement of the operator cost and overhead from the DP algorithm. Due to the high evaluation cost, the optimization time is dominated by the profiling overhead. However, as discussed in §4.2, the repetitive profiling for operator cost can be avoided by saving the cost of each operator. When the cost of every operator is profiled in advance, our op-level placement optimization takes less than a minute on all of the five

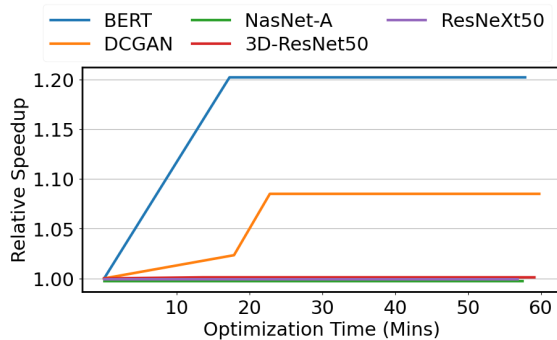


Figure 10. Performance improvement of graph-level placement optimization over time. The y-axis presents the speedup relative to the op-level placement optimization.

networks.

Figure 10 exhibits how our graph-level placement optimization gradually improves from the op-level placement optimization over time. The evolutionary searcher could boost the performance by leveraging more cross-kernel optimizations as it goes through several generations of mutations and crossovers. In BERT and DCGAN, the effect of cross-kernel optimization is quite notable and thus, our graph-level placement optimizer accelerate its execution by 1.09 – 1.20× from the op-level optimization. For the rest of the workloads, graph-level placement optimization cannot improve any further since the placement from the op-level optimization is already hard to beat. Overall, most of workloads are observed to reach the saturation within thirty minutes.

Due to the lack of the efficient cost model that can factor in the cross-kernel optimization effect, graph-level placement optimization has expensive evaluation overhead that leads to the longer optimization time compared to the op-level. Given that our op-level placement optimizer can identify high-performance backend placement for the most workloads within just a minute, we recommend the graph-level placement optimization as the optional tool for the users interested in squeezing the last drop of performance.

6.4 Backend Ablation Study

To assess the impact of integrating backends, we conduct an ablation study by adding backends one-by-one to *Collage*.

Figure 11 shows the experimental result on V100. Overall, *Collage* monotonically improves performance as we integrate more backends. This reinforces the importance of smart mixed-use of multiple backends and also corroborates the robustness of our backend placement optimization. Interestingly, the performance improvement from a new backend varies depending on a network. In the case of BERT and DCGAN, we see relatively consistent enhancement from

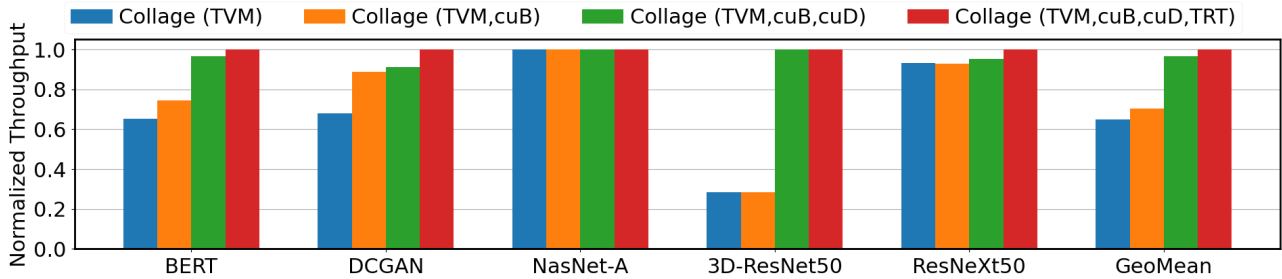


Figure 11. End-to-end performance of *Collage* with different number of backends on NVIDIA Tesla V100. Each throughput is normalized by the throughput of *Collage* (TVM,cuB,cuD,TRT). TVM, cuB, cuD, and TRT represents TVM, cuBLAS, cuDNN, and TensorRT.

each backend. This is because *Collage* identifies a way to utilize every backend for the different part of the workload depending on its own unique strength. In case of NasNet-A and ResNeXt50, TVM offers the majority of the performance improvement while cuDNN significantly benefits *Collage* for the 3D-ResNet50.

These observations show that *Collage* can stably improve performance by having more backends. By leveraging the unique strength of available backends, our automated solution delivers the performance with a set of backends that surpasses or guarantees the performance with its subset.

6.5 Case Study of Backend Operator Placement

To understand the source of performance improvement from *Collage*, we examine two representative workloads in detail. Figure 12 illustrates *Collage*'s final backend placement for ResNeXt50 and BERT on V100.

Even within a single network, we observe that the same type of operator is mapped to different backends due to the performance diversity depending on its configuration, such as data shape and kernel size, and the operator fusion with its neighbor nodes. For example, batch matrix multiplication operators in BERT are assigned to two different backends (cuBLAS and TVM) while convolution operators in ResNeXt50 are assigned to three different backends (cuDNN, TVM, and TensorRT). Interestingly, the graph inference library (e.g., TensorRT) can be a competitive choice even for a single operator as observed with some convolution operators in ResNeXt50.

This figure also demonstrates that *Collage* is capable of leveraging various fusion patterns from each backend. For instance, we discover a variety of operator fusion patterns selected by *Collage* such as Conv+ReLU, Conv+Add+ReLU, and Add+ReLU. Although it is omitted from this figure for simplicity, we observe the fusion pattern involved with more than ten operators. Again, as in a single operator, *Collage* chooses the different backends for the identical fusion pattern of Conv+Relu in ResNeXt50 because the best backend

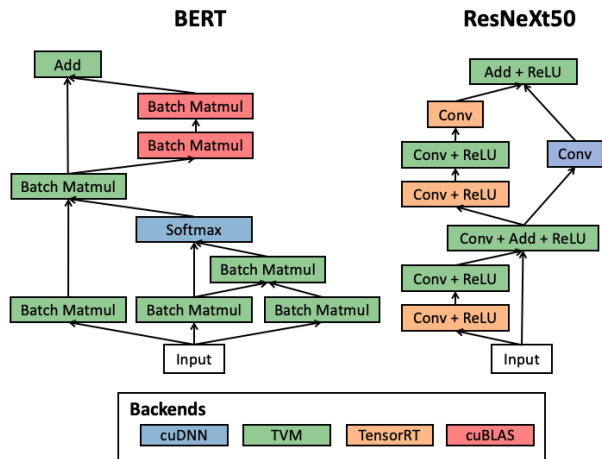


Figure 12. Representative backend placements discovered by *Collage* on V100 (Figure 7a). Note that *Collage* leverages various backends given their unique strength to enhance performance.

choice varies depending on specific operator configurations.

This study confirms that *Collage* can accelerate DL workload execution by leveraging diverse operator patterns from multiple backends given their performance characteristics.

7 CONCLUSION

This work investigated efficient DL backend integration system, called *Collage*. For the integration of various backends, *Collage* offers an user interface that allows the flexible specification of diverse backend capabilities. To find the best uses of available backends, *Collage* introduces a two-level optimization method and automatically customizes the best possible backend placement for the underlying execution environment. The experimental results demonstrate that *Collage* outperforms the manual approach in the state-of-the-arts DL framework by up to $1.40\times$ on average over real-life DL models and various hardware architectures.

REFERENCES

- Apple neural engine (ane). <https://www.apple.com/newsroom/2020/11/apple-unleashes-m1/>. Accessed: 2021-08-25.
- Nvidia deep learning accelerator (nvdl). <http://nvdla.org/>. Accessed: 2021-08-25.
- Intel onednn. <https://software.intel.com/content/www/us/en/develop/tools/oneapi/components/onednn.html#gs.9zgc55>. Accessed: 2021-09-27.
- Intel openvino. <https://software.intel.com/content/www/us/en/develop/tools/openvino-toolkit.html>. Accessed: 2021-09-27.
- Nvidia tensorrt. <https://developer.nvidia.com/tensorrt>. Accessed: 2021-08-05.
- Tensorflow xla. <https://www.tensorflow.org/xla>. Accessed: 2021-09-27.
- Nvidia cublas. <https://developer.nvidia.com/cublas>. Accessed: 2021-08-05.
- Abadi, M., Barham, P., Chen, J., Chen, Z., Davis, A., Dean, J., Devin, M., Ghemawat, S., Irving, G., Isard, M., et al. Tensorflow: A system for large-scale machine learning. In *12th {USENIX} symposium on operating systems design and implementation ({OSDI} 16)*, pp. 265–283, 2016.
- Adams, A., Ma, K., Anderson, L., Baghdadi, R., Li, T., Gharbi, M., Steiner, B., Johnson, S., Fatahalian, K., Durand, F., and Ragan-Kelley, J. Learning to optimize Halide with tree search and random programs. *ACM Trans. Graph.*, 38(4):121:1–121:12, 2019.
- Baghdadi, R., Ray, J., Romdhane, M. B., Del Sozzo, E., Akkas, A., Zhang, Y., Suriana, P., Kamil, S., and Amarasinghe, S. Tiramisu: A polyhedral compiler for expressing fast and portable code. In *2019 IEEE/ACM International Symposium on Code Generation and Optimization (CGO)*, pp. 193–205. IEEE, 2019.
- Chen, T., Moreau, T., Jiang, Z., Zheng, L., Yan, E., Shen, H., Cowan, M., Wang, L., Hu, Y., Ceze, L., et al. {TVM}: An automated end-to-end optimizing compiler for deep learning. In *13th {USENIX} Symposium on Operating Systems Design and Implementation ({OSDI} 18)*, pp. 578–594, 2018.
- Chetlur, S., Woolley, C., Vandermersch, P., Cohen, J., Tran, J., Catanzaro, B., and Shelhamer, E. cudnn: Efficient primitives for deep learning. *arXiv preprint arXiv:1410.0759*, 2014.
- Cyphers, S., Bansal, A. K., Bhiwandiwala, A., Bobba, J., Brookhart, M., Chakraborty, A., Constable, W., Convey, C., Cook, L., Kanawi, O., et al. Intel ngraph: An intermediate representation, compiler, and executor for deep learning. *arXiv preprint arXiv:1801.08058*, 2018.
- Devlin, J., Chang, M.-W., Lee, K., and Toutanova, K. Bert: Pre-training of deep bidirectional transformers for language understanding. *arXiv preprint arXiv:1810.04805*, 2018.
- Fang, J., Shen, Y., Wang, Y., and Chen, L. Optimizing dnn computation graph using graph substitutions. *Proceedings of the VLDB Endowment*, 13(12):2734–2746, 2020.
- Fegade, P., Chen, T., Gibbons, P., and Mowry, T. Cortex: A compiler for recursive deep learning models. *Proceedings of Machine Learning and Systems*, 3, 2021.
- Fortin, F.-A., De Rainville, F.-M., Gardner, M.-A. G., Parizeau, M., and Gagné, C. Deap: Evolutionary algorithms made easy. *The Journal of Machine Learning Research*, 13(1):2171–2175, 2012.
- Goodfellow, I., Pouget-Abadie, J., Mirza, M., Xu, B., Warde-Farley, D., Ozair, S., Courville, A., and Bengio, Y. Generative adversarial networks. *Communications of the ACM*, 63(11):139–144, 2020.
- Hara, K., Kataoka, H., and Satoh, Y. Can spatiotemporal 3d cnns retrace the history of 2d cnns and imagenet? In *Proceedings of the IEEE Conference on Computer Vision and Pattern Recognition (CVPR)*, pp. 6546–6555, 2018.
- He, K., Zhang, X., Ren, S., and Sun, J. Deep residual learning for image recognition. In *Proceedings of the IEEE conference on computer vision and pattern recognition*, pp. 770–778, 2016.
- Jia, Z., Padon, O., Thomas, J., Warszawski, T., Zaharia, M., and Aiken, A. Taso: optimizing deep learning computation with automatic generation of graph substitutions. In *Proceedings of the 27th ACM Symposium on Operating Systems Principles*, pp. 47–62, 2019a.
- Jia, Z., Thomas, J., Warszawski, T., Gao, M., Zaharia, M., and Aiken, A. Optimizing dnn computation with relaxed graph substitutions. *SysML 2019*, 2019b.
- Jouppi, N. P., Young, C., Patil, N., Patterson, D., Agrawal, G., Bajwa, R., Bates, S., Bhatia, S., Boden, N., Borchers, A., et al. In-datacenter performance analysis of a tensor processing unit. In *Proceedings of the 44th annual international symposium on computer architecture*, pp. 1–12, 2017.

- Khan, J., Fultz, P., Tamazov, A., Lowell, D., Liu, C., Melesse, M., Nandhimandalam, M., Nasyrov, K., Perminov, I., Shah, T., et al. Miopen: An open source library for deep learning primitives. *arXiv preprint arXiv:1910.00078*, 2019.
- Lattner, C., Amini, M., Bondhugula, U., Cohen, A., Davis, A., Pienaar, J., Riddle, R., Shpeisman, T., Vasilache, N., and Zinenko, O. Mlir: Scaling compiler infrastructure for domain specific computation. In *2021 IEEE/ACM International Symposium on Code Generation and Optimization (CGO)*, pp. 2–14. IEEE, 2021.
- Niu, W., Guan, J., Wang, Y., Agrawal, G., and Ren, B. Dnnfusion: accelerating deep neural networks execution with advanced operator fusion. In *Proceedings of the 42nd ACM SIGPLAN International Conference on Programming Language Design and Implementation*, pp. 883–898, 2021.
- Paszke, A., Gross, S., Massa, F., Lerer, A., Bradbury, J., Chanan, G., Killeen, T., Lin, Z., Gimelshein, N., Antiga, L., et al. Pytorch: An imperative style, high-performance deep learning library. *Advances in neural information processing systems*, 32:8026–8037, 2019.
- Radford, A., Metz, L., and Chintala, S. Unsupervised representation learning with deep convolutional generative adversarial networks. *arXiv preprint arXiv:1511.06434*, 2015.
- Ragan-Kelley, J., Barnes, C., Adams, A., Paris, S., Durand, F., and Amarasinghe, S. Halide: a language and compiler for optimizing parallelism, locality, and recomputation in image processing pipelines. *Acm Sigplan Notices*, 48(6): 519–530, 2013.
- Roesch, J., Lyubomirsky, S., Weber, L., Pollock, J., Kirisame, M., Chen, T., and Tatlock, Z. Relay: A new ir for machine learning frameworks. In *Proceedings of the 2nd ACM SIGPLAN International Workshop on Machine Learning and Programming Languages*, pp. 58–68, 2018.
- Rotem, N., Fix, J., Abdulrasool, S., Catron, G., Deng, S., Dzhabarov, R., Gibson, N., Hegeman, J., Lele, M., Levenstein, R., et al. Glow: Graph lowering compiler techniques for neural networks. *arXiv preprint arXiv:1805.00907*, 2018.
- Wang, E., Zhang, Q., Shen, B., Zhang, G., Lu, X., Wu, Q., and Wang, Y. Intel math kernel library. In *High-Performance Computing on the Intel® Xeon Phi™*, pp. 167–188. Springer, 2014.
- Xie, S., Girshick, R., Dollar, P., Tu, Z., and He, K. Aggregated residual transformations for deep neural networks. In *Proceedings of the IEEE Conference on Computer Vision and Pattern Recognition (CVPR)*, July 2017.
- Yang, Y., Phothilimtha, P. M., Wang, Y. R., Willsey, M., Roy, S., and Pienaar, J. Equality saturation for tensor graph superoptimization, 2021.
- Zheng, L., Jia, C., Sun, M., Wu, Z., Yu, C. H., Haj-Ali, A., Wang, Y., Yang, J., Zhuo, D., Sen, K., Gonzalez, J. E., and Stoica, I. Anso: Generating high-performance tensor programs for deep learning. In *14th USENIX Symposium on Operating Systems Design and Implementation (OSDI)*, 2020a.
- Zheng, Z., Zhao, P., Long, G., Zhu, F., Zhu, K., Zhao, W., Diao, L., Yang, J., and Lin, W. Fusionstitching: boosting memory intensive computations for deep learning workloads. *arXiv preprint arXiv:2009.10924*, 2020b.
- Zoph, B., Vasudevan, V., Shlens, J., and Le, Q. V. Learning transferable architectures for scalable image recognition. 2018. URL <https://arxiv.org/pdf/1707.07012.pdf>.